The Journal of Experimental Biology 210, 2489-2500
Published by The Company of Biologists 2007
doi:10.1242/jeb.006361

Properties and possible function of a hyperpolarisation-activated chloride current in *Drosophila*

Uwe Rose[1,*], Christian Derst[2], Mario Wanischeck[1], Christiane Marinc[1] and Christian Walther[3]

[1]*Institute of Neurobiology, University Ulm, Albert-Einstein-Allee 11, Ulm 89160, Germany,* [2]*Institute for Integrative Neuroanatomy, Charite, Berlin, Germany and* [3]*Institute of Physiology and Pathophysiology, Philipps University Marburg, Marburg, Germany*

*Author for correspondence (e-mail: uwe.rose@uni-ulm.de)

Accepted 2 May 2007

Summary

A chloride current, $I_{Cl,H}$, slowly activating on hyperpolarisation was investigated in *Drosophila melanogaster* larval muscles using the two-electrode voltage clamp. Sizeable currents were observed after the intracellular chloride concentration ($[Cl^-]_i$) had been elevated by diffusion of Cl^- from the electrodes. The time course of $I_{Cl,H}$ was rather variable and required two exponentials to be accurately described. The reversal potential, –40 to –20 mV in Cl^--loaded fires, shifted on lowering external $[Cl^-]$ in the positive direction. Steady-state activation of $I_{Cl,H}$ was characterised by $V_{0.5}$ of ≈–120 mV and a slope factor, k, of ≈10 mV at a $[Cl^-]_i$ ≈35 mmol l^{-1}. Raising $[Cl^-]_i$ to ≈50 mmol l^{-1} caused a negative shift of $V_{0.5}$ equivalent to the change of E_{Cl} and led to a nearly threefold increase in maximal steady-state conductance. $I_{Cl,H}$ was resistant to 10 mmol l^{-1} Zn^{2+} and 1 mmol l^{-1} Cd^{2+} but was greatly reduced by 1 mmol l^{-1} 9-anthracenecarboxylic acid (9-AC). $I_{Cl,H}$ was affected by changes of extracellular pH and increased on lowering extracellular osmolality. 9-AC also decreased muscle fibre resting conductance by approximately 20% and increased muscle contractions. Reverse transcriptase-polymerase chain reaction (RT-PCR) analysis confirmed the expression of all three ClC genes in muscle, and immunohistochemistry indicated location of *Drosophila melanogaster* chloride channel-2 (DmClC-2) at the Z-lines. We conclude that DmClC-2 accounts for the channels underlying $I_{Cl,H}$, and in part for the resting chloride conductance. DmClC-2 may serve general homeostatic mechanisms such as pH- and osmo-regulation or may support muscle function on high motor activity or during a particular neurohormonal state of the animal.

Supplementary material available online at
http://jeb.biologists.org/cgi/content/full/210/14/2489/DC1

Key words: ClC-2, chloride current, homeostasis, cellular excitation, *Drosophila*.

Introduction

Chloride channels of the ClC family (Jentsch et al., 1993) serve a wide range of functions in the plasmalemma as well as in the membranes of organelles (e.g. Jentsch et al., 2002; George et al., 2001; Suzuki et al., 2006). In skeletal muscle of vertebrates ClC-1 channels activate on depolarisation (Steinmeyer et al., 1991a; Steinmeyer et al., 1991b) and are important regulators of excitability (Koch et al., 1992; Jurkat-Rott and Lehmann-Horn, 2004; Pedersen et al., 2005). This becomes particularly obvious in certain genetically determined muscle diseases in which the function of these Cl^- channels is impaired (e.g. Fahlke et al., 1995; Jentsch et al., 1995; Pusch, 2002). ClC-2 channels activate on hyperpolarisation (Thiemann et al., 1992) and are expressed in a wide range of tissues. These channels seem to serve a variety of functions, such as Cl^- transport, pH- and osmo-regulation, and also seem to be involved in developmental and functional support of certain epithelia (Jentsch et al., 2002; Strange, 2002). In certain mammalian neurons they play a supportive role for Cl^--mediated synaptic inhibition (Staley, 1994; Staley et al., 1996).

In invertebrates, knowledge of those Cl^- channels that are not gated by ligands is fairly restricted. Cl^- conductances that slowly activate upon hyperpolarisation have been observed first in skeletal muscle of crayfish (Reuben et al., 1962) and were subsequently characterised in a neuron of the marine slug *Aplysia* (Chesnoy-Marchais, 1983) and in locust skeletal muscle (Walther and Zittlau, 1998). The types of channels involved have yet to be identified in any of these examples (cf. Wicher et al., 2001). Several ClC channels that activate on hyperpolarisation have been identified and partly characterised in the nematode *Caenorhabditis elegans* (e.g. Petalcorin et al., 1999; Schriever et al., 1999; Nehrke et al., 2000; Rutledge et al., 2001). In the fruit fly *Drosophila melanogaster*, there is only a single gene coding for a plasma membrane ClC channel. According to homology to mammalian ClCs, two additional organellar ClC genes have been identified (Littelton and Ganetzky, 2000) (see Figs S1, S2 in supplementary material). The sequence of the plasma membrane ClC is clearly related to that of mammalian ClC-2, and it has been dubbed *Drosophila melanogaster* chloride channel-2 (DmClC-2)

because the currents obtained on heterologous expression resemble those carried by mammalian ClC-2 channels (Flores et al., 2006).

The neuromuscular system of the fruit fly *Drosophila* has evolved as one of the standard models for studies of synaptic and non-synaptic aspects of excitability (Jan and Jan, 1976; Wu and Haugland, 1985; Gho and Mallart, 1986; Elkins and Ganetzky, 1988; Atwood et al., 1993; Kidokoro and Nishikawa, 1994; Tsunoda and Salkoff, 1995; Gielow et al., 1995; Singh and Wu, 1999). Several muscular cation channels have been determined and characterised (reviewed in Wicher et al., 2001), but so far no non-synaptic Cl^- current has been described for this preparation. The presence of a muscular Cl^- conductance (cf. Bretag, 1987), however, would be expected, which may act in concert with some K^+ conductance(s) and ion transporters in order to regulate the muscle fibre's internal milieu. We here give a first account of a hyperpolarisation-activated Cl^- current ($I_{Cl,H}$) in *Drosophila* larval muscles that seems to be carried by DmClC-2.

Materials and methods

Preparation and solutions for electrophysiology

For two-electrode voltage-clamp measurements, wandering third-instar larvae were washed and dissected as described previously (Jan and Jan, 1976). In brief, larvae were fixed dorsal side-up with stainless steel needles. An incision was made along the dorsal midline and the body walls were pinned down laterally. The gut, malphigian tubules, imaginal discs and nervous system were carefully removed to expose the body wall muscles.

The saline for dissection and voltage-clamp recordings consisted of 45 mmol l^{-1} NaCl, 10 mmol l^{-1} KCl, 20 mmol l^{-1} $MgCl_2$, 0.2 mmol l^{-1} $CaCl_2$, 10 mmol l^{-1} $NaHCO_3$, 10 mmol l^{-1} trehalose, 5 mmol l^{-1} N,N-Bis(2-hydroxyethyl)-2-aminoethane-sulfonic acid (BES), and 115 mmol l^{-1} sucrose. For recordings of synaptic currents the calcium concentration was raised to 1 mmol l^{-1}. The pH of the saline was adjusted to 7.2 with NaOH or HCl. During the recordings the preparation was superfused with saline at a constant rate of ≈1 ml min^{-1}. The bath temperature was 20±2°C.

In those experiments in which the membrane voltage was stepped to voltages more positive than –20 mV (so that potassium currents were activated; Figs 4, 5), the saline contained 20 mmol l^{-1} tetraethylammonium (TEA), 1 mmol l^{-1} 4-aminopyridine (4-AP), and 0.1 mmol l^{-1} quinidine with sucrose reduced to 95 mmol l^{-1}. When the chloride concentration was reduced, Na-gluconate was used as a substitute. Hypotonic saline was made by lowering the sucrose concentration. To test the effect of 5-nitro-2-(3-phenylpropylamino) benzoic acid (NPPB) and 4,4′-diisothiocyanatostilbene-2,2′-dilsulfonic acid (DIDS) on the chloride current, these drugs were dissolved in dimethyl sulfoxide (DMSO), which caused membrane instabilities even at the very low concentration of 0.05 vol%. Whenever DMSO was in the bath, measurements were frustrated by suddenly occurring leaks. The drug 9-anthracenecarboxylic acid (9-AC; Sigma, Munich, Germany), however, could be dissolved in DMSO-free saline by means of sonication up to a concentration of 1 mmol l^{-1}.

Electrophysiology

Voltage and current electrodes were pulled from thin-walled borosilicate glass (outer and inner diameter: 1 mm and 0.78 mm, respectively; Harvard Apparatus, March-Hugstetten, Germany) using a Sutter P-97 puller. The voltage electrode was filled with 3 mol l^{-1} KCl. The current electrode contained either 2 mol l^{-1} K-citrate plus 50 mmol l^{-1} KCl or 3 mol l^{-1} CsCl or 3 mol l^{-1} KCl. K-citrate was used to prevent loading of muscle fibres with chloride. CsCl diffusing into the fibre largely suppressed outward potassium currents (Erxleben and Rathmayer, 1997). The resistance of the voltage electrodes was between 13 and 15 MΩ and that of the current electrodes was between 4 and 6 MΩ. Two-electrode voltage-clamp recordings were performed by means of a Turbo TEC-10CX amplifier (NPI, Tamm, Germany) connected to the computer *via* an INT-10 interface (NPI). A 3 mol l^{-1} KCl agar bridge connected the bath to the reference electrode.

Acquired signals were digitised by a 12-bit A/D board (PCI-1200; National Instruments, Austin, TX, USA) at a sampling rate of 10 kHz and stored for subsequent evaluation. Voltage commands were generated by computer software (Cell Works, NPI) through the PCI-1200, 12-bit A/D board. Evaluation of data was done with Igor Pro 5.05 software (Wavemetrics, Inc., Lake Oswego, OR, USA), and figures were prepared with Corel Draw 12.0 (Corel Corporation, Ottawa, Canada) and Igor Pro 5.05.

The current electrode was placed in the center of the fibre and the voltage electrode half-way between the current electrode and one end of the fibre. After inserting the electrodes, the voltage clamp was adjusted so that the capacitive current caused by a rectangular voltage jump settled within less than 3 ms. At the beginning of each recording, the cell capacitance and resistance were measured with a two-ramp protocol according to Walther et al. (Walther et al., 1998). To elicit the chloride current, membrane voltage was stepped in the negative direction in 10 mV increments. The holding potential was –50 mV (unless otherwise stated), which was in the range of the normal resting membrane potential (Ball et al., 2003) and approximately 10 mV below the activation threshold of the hyperpolarisation-activated current. To prevent excessive chloride efflux from the fibre, which preferentially occurs at membrane voltages below –90 mV and may cause changes of the Cl^- equilibrium potential (e.g. Niemeyer et al., 2003), the hyperpolarising pulses were terminated after 2 to 4 s, despite the fact that the currents were not yet fully activated. Therefore, steady-state currents were extrapolated by fitting a bi-exponential equation to the current traces (see below). Reversal potentials of hyperpolarisation-activated currents were determined by a voltage protocol consisting of an activating voltage step to –120 mV for 3 s, followed by a voltage ramp from –50 mV to 0 mV within 50 ms. The same ramp was performed without preceding hyperpolarisation and the currents were then subtracted.

Synaptic currents were elicited by electrical stimulation of the segmental nerve *via* a glass suction electrode. Stimulus strength was supra-maximal to ensure comparable excitation during the course of the experiment.

Ueda and Kidokoro have shown some intersegmental coupling of fibres in the larval preparation (Ueda and Kidokoro, 1996). We did not, however, notice difficulties with clamping. Although the real time courses of the currents may

be somewhat faster and their voltage dependence steeper than measured, our experimental findings are not compromised by fibre coupling.

The basic dissection for tension recordings was as described above. In addition, body wall muscles surrounding muscle 6 and 7 in segment A3 were destroyed with a glass needle to essentially restrict contraction measurements to muscle 6 and 7. Near their anterior insertions, the two muscles were fixed to the dish with insect pins. The cuticle at their posterior end was attached to the lever arm of a force transducer (KG4A; Scientific Instruments, Heidelberg, Germany) mounted on a micromanipulator. The force transducer was connected to a bridge amplifier (BAM 47C, Scientific Instruments). After each series of contractions the preparation was repeatedly superfused with aerated saline. Tension recordings were approximately isometric (deflection of the transducer tongue: 1 nm/1 μN). The response of the transducer was linear over the range used in the experiments and it was calibrated after each experiment. During tetanic stimulation the resulting tension varied over time (Fig. 9A). For this reason the peak tension was measured and evaluated.

Data analysis

To estimate the activation and deactivation parameters, current traces were fitted to a bi-exponential equation:

$$I_{Cl,H}(t) = A_0 + A_1(1-e^{-t/\tau_1}) + A_2(1-e^{-t/\tau_2}) , \quad (1)$$

which yielded steady-state currents (A_1, A_2) and time constants (τ_1, τ_2). The parameter A_0 represents a possible current offset. Conductances were fitted using a Boltzmann distribution of the form:

$$G = G_{max} / 1+\exp[(V-V_{0.5})/k] , \quad (2)$$

where G and G_{max} are conductances, $V_{0.5}$ the voltage at which activation is half-maximal and k the slope factor. There may be a voltage-independent component of the chloride conductance [G_0 in Flores et al. (Flores et al., 2006); see also Discussion], which, however, was not looked for because it seemed not possible to determine such a component reliably. Even in the presence of a mix of blocking agents, one has to expect residual and probably hitherto unknown currents in this muscle preparation. However, there might already be some voltage-dependent activation of the channels at the holding potential (–50 mV) and at the membrane voltage at which tail currents were measured (–60 mV). The investigation using the above protocols would then determine the increases in activation induced at more negative voltages rather than the total amount of voltage-dependent activation. This possibility was tested in four independent experiments in which we stepped to negative voltages from a holding potential of –20 mV. A voltage-dependent activation was reliably noticed only at potentials negative to –50 mV.

According to the method described by Walther et al. (Walther et al., 1998)[†], a possible voltage-dependent activation was also tested for in several examples by fitting to the conductances a double Boltzmann equation of the form:

$$G=G_{max}/1+\exp[(V-V_{0.5})/k)]-G_{max}/1+\exp[(V_t-V_{0.5})/k)] , \quad (3)$$

where V_t is the voltage at which the tail currents were measured. Our evaluation of three experiments revealed an indication for a slight activation (1–3% of G_{max}) at the test potential of –60 mV.

The data are given as mean and their standard errors (s.e.m.). The number of larvae (l) and muscle fibres (f) used in the experiment are given in the text. Statistical significance was determined by parametric tests (paired or unpaired *t*-test) and assumed for $P<0.05$.

Preparation of Drosophila tissues for expression studies

Reverse transcriptase-polymerase chain reactions (RT-PCRs) were performed as described recently (Derst et al., 2006). In brief, central nervous systems (CNSs) from wandering third-instar larvae (*white* w^{1118}, kindly provided by R. Hyland, Institute of Developmental Biology, Department of Biology, University of Marburg, Germany) were collected by tearing the larvae apart. CNSs were cleaned from adherent organs, including the imaginal discs. Each CNS was immediately transferred into an Eppendorf vial kept within a metal block on dry ice. Collected CNSs or body wall preparations were kept at –80°C for storage.

We also developed an approach to obtain pure muscular tissue (‘pure muscle preparation’), based on a procedure originally devised for protein studies (Fujita et al., 1987). Larvae were pinned to small silicon discs and the internal tissue except for the muscles was removed under standard *Drosophila* saline (see below) or Schneider’s *Drosophila* Medium (Gibco/Invitrogen, Karlsruhe, Germany). The body walls were then kept on ice for up to 2 h. A glass flask containing acetone and 9 g/100 ml anhydrous Na_2SO_4 was put into liquid N_2 and the preparations were then transferred into the freezing acetone. The acetone flask was subsequently put into a –25°C freezer and left there for at least 15 h (up to several weeks). For collecting dried muscle fibres, a body wall preparation was transferred from the silicone support into the lid of an Eppendorf vial and secured with two steel needles. Muscle fibres were gently prodded and dislocated with fine forceps or with a needle. The isolated fibres were electrostatically transferred to the supporting lid to which they remained firmly stuck so that the collection of fibres gained from one preparation could be saved with this lid to perform RT-PCRs.

RT-PCR analysis of Drosophila ClC channel expression

RNAs from *Drosophila* muscle fibres and CNSs were isolated using the RNeasy RNA mini kit (Qiagen, Hilden, Germany) and were reverse transcribed using the Sensiscript Reverse Transcriptase Kit (Qiagen). For each of the three *Drosophila melanogaster* ClC channels two pairs of PCR primers were designed. To distinguish between genomic DNA and cDNA sequences, primers were located on different exons, which leads to considerably larger PCR products, in case of genomic DNA amplifications. The following primers were designed (the size of RT-PCR and genomic PCR product is indicated in brackets): DmClCa F1-B1 (520/1180 bp) 5′-TCATCATGGACAAGGGCATA-3′ and 5′-AGAATCCGCG-

[†]In the joint publications of Walther et al. (Walther et al., 1998) and Walther and Zittlau (Walther and Zittlau, 1998), there is a typing error in all Boltzmann equations. Instead of ‘…(1–exp[(V–$V_{0.5}$)/S])’, the term should read ‘…(1+exp [(V–$V_{0.5}$)/S])’.

CCAGTAGTTA-3′; DmClCa F2-B2 (350/970 bp) 5′-TCTGACGTCACAGCCTTTTG-3′ and 5′-CCGCCAACATTTCAGAGTTT-3′; DmClCb F1-B1 (590/920 bp) 5′-CGGAACTTTTCGTGACCATC-3′ and 5′-TGGACAAATGCCATGCTTTA-3′; DmClCb F2-B2 (340/770 bp) 5′-CAGCACACCAAACTGACCAC-3′ and 5′-ATCTTCGTACTGCCCAATGC-3′; DmClCc F1-B1 (640/760 bp) 5′-ATTTCACGTTCACGGGTCTC-3′ and 5′-ATGGTCATTCGAAGCACTCC-3′; DmClCc F2-B2 (400/520 bp) 5′-GCAATGATGGGCGTAACTTT-3′ and 5′-GCAGCTCCAATTAGGGCATA-3′.

PCR was performed with Advantage Taq 2 DNA Polymerase Mixture (Clontech, Hamburg, Germany) with 30 s 94°C denaturation, 30 s 55°C annealing and 1 min 68°C elongation for 35 cycles. PCR products were visualised on a 1.5% agarose gel. In addition, PCR products were cloned into pGEM-T vector and sequenced to verify the specificity.

Immunohistochemistry

Immunohistochemical localisation of ClC-2 channels in the muscle membrane essentially followed the protocol described in Ugarte et al. (Ugarte et al., 2005). In brief, larvae were filleted and fixed in 4% paraformaldehyde for 2 h and subsequently washed several times in 0.1 mol l^{-1} phosphate buffer (PB). Incubations in the primary antibody (anti-ClC-2 antibody, 1:400, ACL-002; Alomone Laboratories, Jerusalem, Israel) or antibody preincubated with ClC-2 peptide (1 μg peptide per 1 μg antibody) were performed overnight. After rinsing several times in 0.1 mol l^{-1} PB, preparations were incubated with the secondary antibody (Cy3-conjugated anti-rabbit, 1:1000; Sigma, Germany) for 1 h. The preparations were finally rinsed in PB, mounted on a slide and photographed under a fluorescent microscope equipped with a CCD camera (CCD 1300B; Vosskuehler, Osnabrueck, Germany).

Results

Raising the internal Cl^- concentration augments a hyperpolarisation-activated inward current

When *Drosophila* larval muscle fibres were hyperpolarised the currents measured immediately after stepping the voltage (‘instantaneous currents’; open symbols in Fig. 1) were characterised by a virtually linear current–voltage (*I–V*) relationship. Hyperpolarisations of several seconds evoked an additional inward current that developed slowly and eventually became stationary (Fig. 1B,D, filled symbols). Initially, i.e. ≈1 min after impaling the fibre, this extra inward current was small compared with the instantaneous current (Fig. 1, circles). The inward current did not change significantly with recording time when the current electrode contained 2 mol l^{-1} potassium-acetate (Fig. 1A,B), but clearly increased when the current electrode contained 3 mol l^{-1} KCl (Fig. 1C,D). The instantaneous *I–V* relationship remained linear (Fig. 1D, open squares) whereas that of the currents sampled at the end of a prolonged (4 s) hyperpolarisation exhibited inward rectification (Fig. 1D, filled squares). The hyperpolarisation-dependent currents did not show signs of inactivation with commands lasting five times longer than those in Fig. 1 (not shown). Their final sizes (i.e. >10 min after impalement) were rather variable.

The slow inward current that, as shown below, is a Cl^- current, thus appears to be augmented by a rise in internal [Cl^-] because of diffusion of Cl^- ions from the electrodes. Fig. 2A shows examples of full-blown hyperpolarisation-dependent inward currents and pronounced inward tail currents. In current clamp (Fig. 2B) these inward currents lead to slow ‘depolarisations’ (or ‘sags’) after the initial hyperpolarisation. In this way the hyperpolarisation-dependent inward current causes its own, partial deactivation. When the current injection is terminated, the voltage at first ‘overshoots’ and then slowly decays to the initial

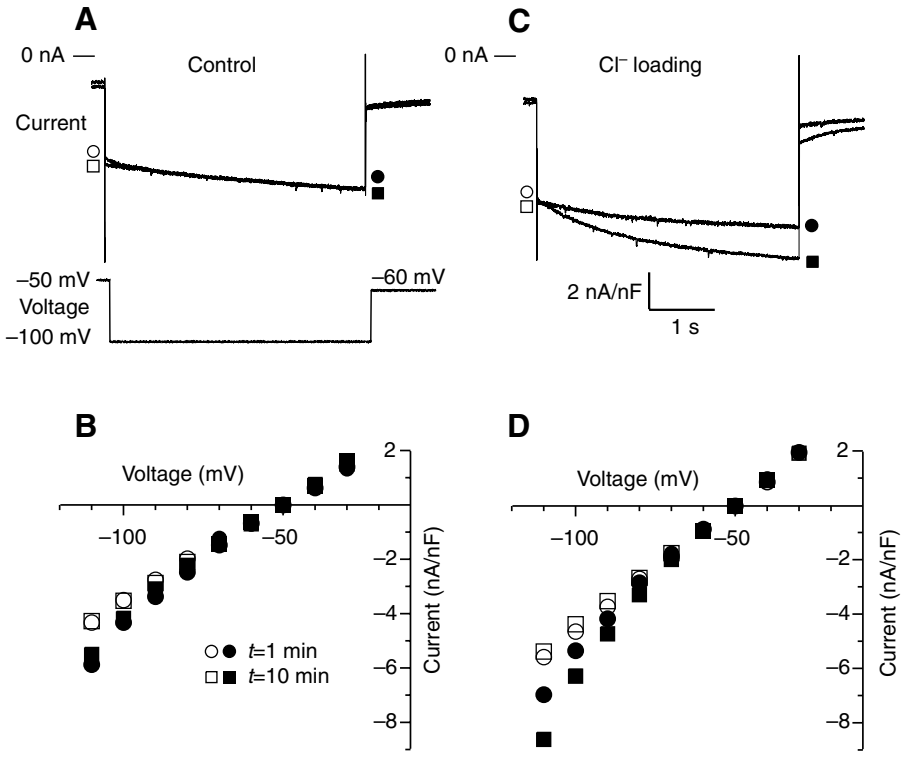

Fig. 1. Currents recorded from a muscle fibre during prolonged hyperpolarising voltage commands. (A) Current electrode filled with 2 mol l^{-1} K-acetate. After the instantaneous jump, a small inward current develops within seconds. The superimposed traces, recorded 1 and 10 min after impaling the fibre, are nearly identical. Note that the lower trace represents the recorded voltage imposed by the pulse protocol. (B) Current–voltage relationships for the fibre in A. The instantaneous current (open symbols) is linear whereas the late current (filled symbols) exhibits slight inward rectification. (C) Recording from another fibre where current electrode filled with 3 mol l^{-1} KCl was used; voltage jump as in A. Although the current recorded is initially similar to that in A, the slow inward component is clearly increased 10 min after impalement. (D) *I–V* plot for the fibre recorded in C. The instantaneous current is practically linear, as in B, but the inward rectification of the late current is enhanced 10 min after impalement. Note inward-going tail currents after jumping from –110 to –60 mV. In both A and B the voltage electrode contained 3 mol l^{-1} KCl.

membrane potential. This 'rebound' depolarisation reflects the slow deactivation of the inward current.

Ionic nature of the hyperpolarisation-dependent current

The finding that the hyperpolarisation-dependent current is enhanced when intracellular [Cl^-] is elevated beyond the resting level suggests that we are dealing with a Cl^- current like that previously found in locust skeletal muscle (Walther and Zittlau, 1998). In locust skeletal muscle and other insect preparations, however, phenomenologically similar inward currents can also be carried by K^+ channels (Walther et al., 1998; Wicher et al., 2001) or cation channels (Heidel and Pflüger, 2006), which are permeable to both K^+ and Na^+ and which are blocked by Cs^+ [e.g. Pape (Pape, 1996); there is at least one gene in *Drosophila* coding for such a type of channel, cf. Littleton and Ganetzky (Littleton and Ganetzky, 2000)]. We therefore compared the reversal potentials, E_{rev}, of the tails for the hyperpolarisation-dependent inward current and for a depolarisation-dependent K^+ outward current in the same fibre, as shown in Fig. 3A. Under the conditions used for these experiments, the average E_{rev} of the K^+ current was –55.2±4.1 mV, whereas that of the hyperpolarisation-dependent current was –20.5±4.0 mV (average from paired measurements: f=4, l=2; cf. *I–V* plots in Fig. 3B). Application of Cs^+ (1–5 mmol l^{-1}) did not reduce the current.

As would be expected for a Cl^- current, the E_{rev} of the inward tails from the hyperpolarisation-dependent currents became the more positive the longer and stronger a fibre was loaded with Cl^-. Also, when the external Cl^- concentration was lowered from 65 to 20 mmol l^{-1}, E_{rev} changed from –18.2±1.8 mV to +2.2±3.8 mV (Fig. 4; f=3, l=1). This shift was approximately 9 mV less than predicted by the Nernst equation (29.7 mV for a Cl^- current). This discrepancy can be explained by the fact that the fibres lost Cl^- on equilibration with the low-chloride saline, which took 5 to 8 min. Taken together, these findings indicate that the hyperpolarisation-dependent current is in fact a Cl^- current that we subsequently refer to as '$I_{Cl,H}$'.

Current–voltage characteristics and kinetics of the Cl^- current $I_{Cl,H}$

The average *I–V*-relationship of the tail currents (Fig. 3B and Fig. 4) is practically linear, i.e. the conductance of the open channels seems to be voltage-independent over the range investigated. In some of our experiments there appeared to be a slight inward rectification whereas, for a purely ohmic conductance, some outward rectification would be expected.

To investigate the time courses of activation and deactivation, we performed fits to the currents at –120 mV and to the corresponding tail currents at –60 mV (f=9, l=4). The time courses could be described satisfactorily by two exponentials (Eqn 1). The fit parameters varied greatly between fibres. At –120 mV (i.e. for activation) the average values were: τ_1=1.77±0.51 s (range: 0.54–4.69 s); τ_2=3.53±1.28 s (range: 2.19–9.90 s). The amplitude ratio A_1/A_2 also varied considerably, i.e. from 1:1 to 1:4.5, and was on average 1:1.8. Additional figures, obtained from another set of experiments, are displayed in Table 1 (controls). At –90 mV, currents seemed to activate with practically the same time course as at –120 mV. At –60 mV (i.e. on deactivation) A_1/A_2 was 1:2.5 and the time constants were: τ_1=0.51±0.16 (range: 0.21–1.39); τ_2=1.28±0.27 (range: 0.48–2.94). There was no indication that the time courses depended on whether the fibre had already been well-loaded with Cl^-, as was the case for the above figures, or whether they had been only moderately loaded.

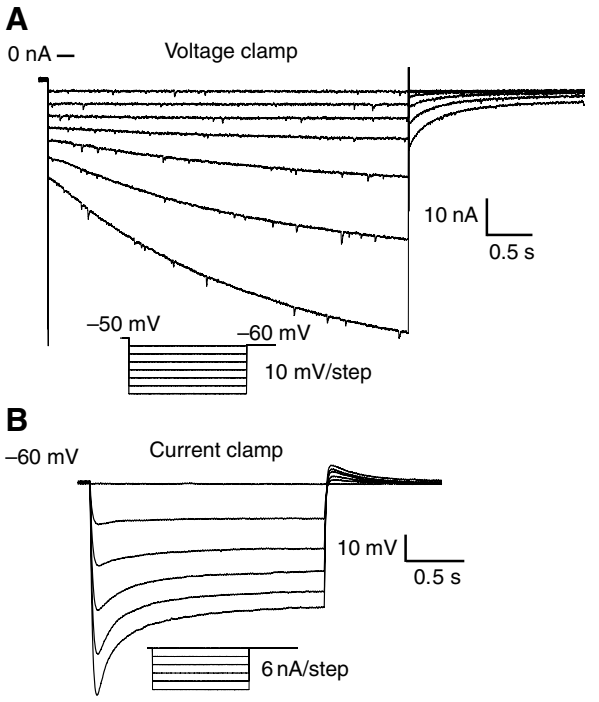

Fig. 2. Hyperpolarisation-induced current in a Cl^--loaded muscle fibre. (A) Currents elicited by the hyperpolarising voltage commands shown in the inset. Note the pronounced tail currents after deactivating jumps to –60 mV. Small, short inward currents are miniature excitatory junctional currents. The recordings were performed after holding the fibre for 5 min at –50 mV with a holding current of ≈–5 nA. The current electrode was filled with 3 mol l^{-1} KCl. (B) Current clamp recordings subsequently performed from the same fibre; currents were injected according to the protocol shown in the inset.

Steady-state activation of $I_{Cl,H}$

The parameters of steady-state activation were determined from the currents induced by hyperpolarising voltage commands and from the reversal potential of $I_{Cl,H}$, which was regarded as the Cl^- equilibrium potential. Measurements in each fibre were performed before and after Cl^- loading. Conductances were fitted using the Boltzmann distribution specified in the Materials and methods section. The activation parameters yielded by the fits are summarised in Table 2.

Activation was absent or small at –60 mV with moderate or strong Cl^- loading, respectively, and saturated at around –180 mV or at more negative voltages (Fig. 5A). The extrapolated maximal conductance dramatically increased as $[Cl^-]_i$ was raised from ≈38 to ≈54 mmol l^{-1}. The increase at –180 mV was almost threefold and could not be solely attributed to the increase in driving force (only ≈6% at –180 mV). In addition, the increase in $[Cl^-]_i$ led to a positive shift of the activation curve on the voltage axis by 13 mV (Fig. 5B), which is similar to the shift of E_{Cl} (≈9 mV; cf. Table 2).

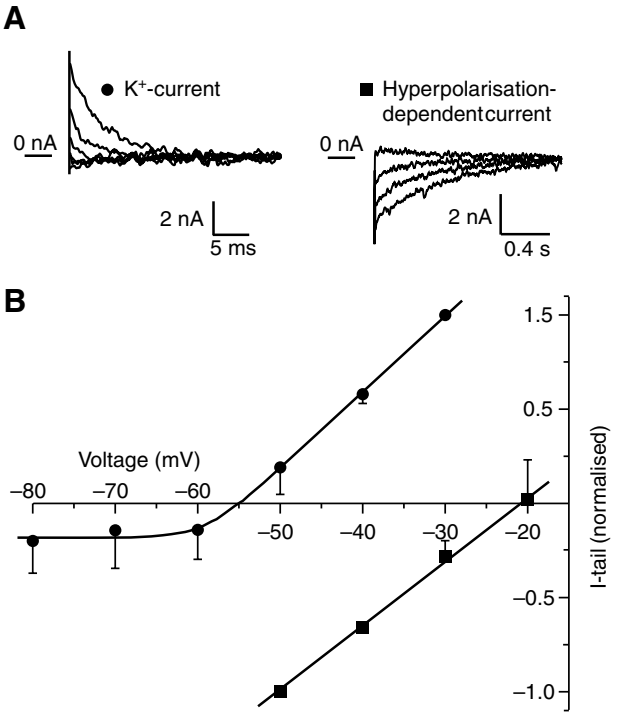

Fig. 3. Reversal potentials of K^+ current and hyperpolarisation-induced current. (A) Sample traces of tail currents recorded subsequently in one fibre. Left: deactivating K^+ currents, mainly consisting of A currents. For K^+ current activation the fibre was first depolarised from –70 to +10 mV for 80 ms, then the voltage was stepped to different levels as seen in B. Right: deactivation of hyperpolarisation-dependent currents. For activation the voltage was stepped from –50 mV to –120 mV for 4 s, followed by deactivating jumps to –50 mV or more positive levels as seen in B. (B) Mean current–voltage relationships of peak tail-currents obtained, as in A, from paired recordings of four fibres from two animals. Note that the ordinate gives relative sizes of the currents, i.e. normalised to I_K at V=–30 mV and to hyperpolarisation-dependent current at –50 mV, respectively. $[K^+]_o$ and $[Cl^-]_o$ were standard, i.e. 10 mmol l^{-1} and 95 mmol l^{-1}, respectively. The mean reversal potential was –55.2±4.1 mV for the K^+ current and –20.5±4.0 mV for the hyperpolarisation-activated current (l=2, f=4). The current electrode contained 3 mol l^{-1} KCl; recordings of the hyperpolarisation-dependent currents were performed 5 to 10 min after impaling the fibre.

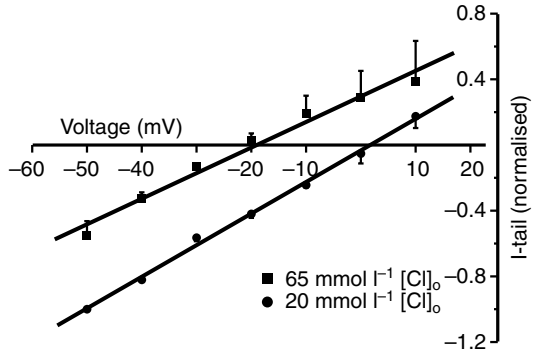

Fig. 4. The reversal potential of the hyperpolarisation-induced current depends on the external Cl^- concentration. Current–voltage relationships of tail currents as shown in Fig. 3A, right-hand side. Averages of paired measurements in three fibres, performed first with $[Cl^-]_o$=65 mmol l^{-1} and then with $[Cl^-]_o$=20 mmol l^{-1}. The reduction of $[Cl^-]_o$ led to a positive shift of the reversal potential, i.e. from –18.2±3.8 mV to +2.2±1.8 mV. K^+ currents were blocked by means of 20 mmol l^{-1} TEA, 1 mmol l^{-1} 4-aminopyridine (4AP) and 0.1 mmol l^{-1} quinidine.

pH dependence of $I_{Cl,H}$

After changing the extracellular pH from 7.2 to 8.4, the amplitude of the fast-current component was reduced by ≈70% at –120 mV, as indicated by the double-exponential fits. At pH 8.4 activation of $I_{Cl,H}$ was faster than at pH 7.2 (Fig. 6A; Table 1). When the pH was changed to 6.0, the current was again reduced (both components by some 70%) whereas the time course was not significantly affected, contrary to the impression one might get from Fig. 6B (see Table 1). Changing the pH from 7.2 to either 8.4 or 6.0 led to immediate effects that were completed within 1 min, whereas the reversal of effects on switching back to pH 7.2 was comparatively slow (not yet complete within 5 min; Fig. 6). The pH changes also affected the tail currents in a manner similar to that observed for the activating currents.

Potentiation of $I_{Cl,H}$ in hypotonic solution

One of the characteristic features of ClC-2 currents is their potentiation by hypotonicity-induced cell swelling (e.g. Jentsch et al., 2002). In hypotonic solutions $I_{Cl,H}$ increased significantly (Fig. 7). For a reduction of osmolality by 33% the increase quantified from tail currents amounted to 350±132% (f=4, l=2; Fig. 7C). The potentiation appeared to be similar for all pre-pulse voltages tested, and Boltzmann fits to the data indicated a major effect on the maximal current (cf. Fig. 7B and legend). The osmotic effect fully reversed within 5 to 8 min (Fig. 7).

Effects of blockers

9-AC

Mammalian ClC-2 currents are known to have characteristic differential susceptibilities to a variety of blockers, and this ‘fingerprint’ is one of the means to test whether or not a native Cl^- current belongs to the ClC-2 subfamily (Jentsch et al., 2002). Of these blockers, 9-AC proved effective in *Drosophila* muscle (Fig. 8). When channels were gated by hyperpolarisation, the block slowly ensued and was released shortly after repolarisation, as tested by subsequent reactivation. We also observed a voltage sensitivity of the 9-AC block, increasing with the level of hyperpolarisation (not shown). With 1 mmol l^{-1} 9-AC in the bath (Fig. 8Ai,Aii), the current measured at the end of a 5 s voltage command reached only 3.9±3% of the control (f=4, l=2). Washing with saline almost completely reversed the 9-AC block (104±8%, f=3, l=2). 9-AC also affected the resting conductance of muscle cells (Fig. 8B). Compared with controls, membrane conductance was lowered within 3 min after 9-AC application to 87.5±4.1% (f=7, l=7). Subsequent washing increased the resting conductance to 124.1±10.5% (f=6, l=6). We also determined the influence of 9-AC on stimulus-evoked postsynaptic currents (epsc) in four larvae (Fig. 8C). 1 mmol l^{-1} 9-AC consistently reduced epscs in all experiments to approximately 70% of the control current. This effect was reversed by washing with *Drosophila* saline.

The effect of 9-AC on resting conductance raised the question

Table 1. *$I_{Cl,H}$ time course and amplitude dependence on extracellular pH*

	τ_1 (s)	τ_2 (s)	A_1 (nA)	A_2 (nA)
Control	2.9±0.6	4.3±1.0	25.3±7.3	28±7.8
Percentage of control				
pH 8.4	11±3.6	29±7.5	30±14.7	79±21.0
Wash	87±17.5	73±11.2	56±13.2	78±16.9
Control	3.5±0.7	3.7±0.7	13.4±3	13±3.7
Percentage of control				
pH 6.0	99±32.0	105±35.1	27±6.2	27±7.4
Wash	79±11.0	96±12.4	87±7.3	104±11.3

Means ± s.e.m.; l=3, f=5.

Table 2. *Effects of intracellular Cl^- concentration on activation of $I_{Cl,H}$*

	E_{Cl} (mV)[b]	$[Cl^-]_i$ (mmol l^{-1})[c]	$V_{0.5}$ (mV)	k (mV)	G_{max} (μS)
Pre-loading[a]	–28±1.1	36.2–39.5	–119±4.7	–10.2±1.7	–0.28±0.1
Post-loading[a]	–19±1.4	51.2–57.2	–106±2.8	–11.3±1.6	–0.67±0.1
			P<0.05	n.s.	P<0.05

[a]Paired current measurements were performed in six muscle fibres, i.e. ≈1 min after impalement and ≈4 min later. Because of diffusion of Cl^- ions from the electrodes (cf. Materials and methods), the intracellular Cl^- concentration $[Cl^-]_i$ was initially slightly ('pre-loading') and then strongly elevated ('post-loading').

[b]According to the reversal potential of $I_{Cl,H}$.

[c]Calculated from E_{Cl} according to the Nernst equation (Cl_o=115 mmol l^{-1}). Values represent ranges. n.s., not significant.

of how altered chloride-channel conductance would influence muscle contractions. To experimentally address this question, we applied 9-AC and measured neurally evoked contractions (Fig. 9A). In all of 10 experiments, contractions measured in the presence of 1 mmol l^{-1} 9-AC were significantly increased (Fig. 9A,B). This effect was reversed by removing 9-AC from the bath. The effect of 9-AC was similar for twitch as well as tetanic contractions (5 Hz, 10 Hz). The kinetics of twitch contractions (50% relaxation time) were not significantly changed.

Other blockers

For technical reasons (cf. Materials and methods), stilbene derivatives and NPPB could not be properly tested. Inorganic ions such as barium (10 mmol l^{-1}), cadmium (1 mmol l^{-1}), cesium (10 mmol l^{-1}) and zinc (10 mmol l^{-1}) were tested and showed no significant effect on the $I_{Cl,H}$. Barium was found to effectively block a hyperpolarisation-activated potassium current in locust muscle ($I_{K,H}$) (Walther et al., 1998), and cesium is known to block a hyperpolarisation-activated cation current (I_h) (Zhang et al., 2003). Hence, the ineffectiveness of these blockers ruled out the possibility that the hyperpolarisation-activated current in *Drosophila* muscle represents a mixed current.

Neuromuscular expression of ClC genes

Expression of ClC genes in larval CNS and muscle tissue was investigated by RT-PCR. The *Drosophila* genome contains three ClC genes, each of which corresponds to a different branch of the mammalian ClC channel family (e.g. Jentsch et al., 2002) (cf. also Fig. S1 in supplementary material). To avoid confusion with the mammalian ClC nomenclature, *Drosophila* ClC genes in Fig. 10 and also in the supplementary material were labelled 'DmClC-a', 'DmClC-b' and 'DmClC-c'. The gene DmClC-a corresponds to the mammalian ClC-2. The *Drosophila* terms refer to the FlyBase numbers *CG31116* (DmClC-a), *CG8594* (DmClC-b) and *CG5284* (DmClC-c).

PCR analyses in body wall preparations (Fig. 10A) showed significant expression of all three DmClCs. The results were consistent with both primer sets (cf. Materials and methods) tested for each DmClC channel. In addition, larger genomic PCR fragments were amplified in all PCR reactions. This is not surprising as genomic contaminations of RNA samples cannot be prevented and introns in *Drosophila* genes are very small. The expression of all three DmClC channels was also observed in the CNS (only shown for DmClC-a, Fig. 10B). At least for DmClC-a, this finding is not unexpected in view of its close relation to mammalian ClC-2, which occurs in so many different tissues (e.g. Jentsch et al., 2002). Fig. 10B provides strong proof that DmClC-a is in fact expressed in muscle (four out of five trials) and not, as is theoretically possible, just in some non-muscular tissue of the body wall. Muscular expression was also consistently observed for DmClC-b (five out of five preparations), whereas for DmClC-c channels only a very weak signal was found in two out of five preparations (not shown).

To locate the DmClC-a ion channel in muscle fibres we used an antibody raised against a rat ClC-2 gene product (accession no. P35525). This antibody has already been used in studies of *Drosophila* photoreceptors (Ugarte et al., 2005). Our immunohistochemical experiments showed a strong signal that was strictly associated with the Z-line of the sarcomere

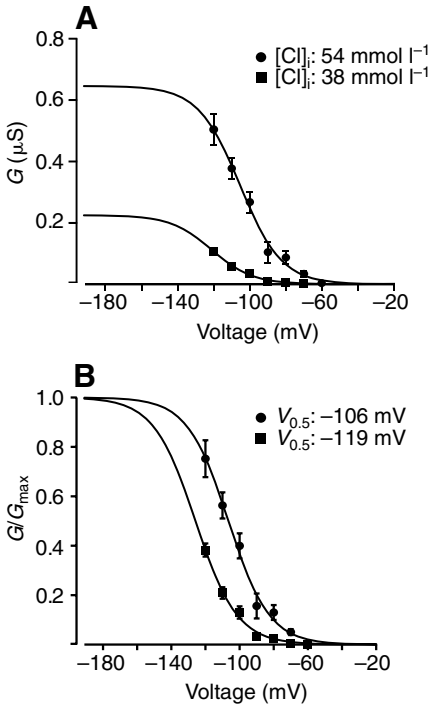

Fig. 5. Steady-state activation of the chloride-conductance, $G_{Cl,H}$. (A) Mean *G–V* relationship at two different internal Cl^- concentrations. Paired measurements of currents and of E_{Cl} were performed in six fibres after moderate and strong Cl^- loading of the fibre (the respective recordings were performed 1 and 5 min after impalement; for details of the approach and for the voltage-clamp protocols employed, cf. Materials and methods). Currents were converted to conductance, *G*. The conductance is greatly enhanced at raised $[Cl^-]_i$. This effect is largely because of the increase in maximal conductance. (B) Normalised *G–V* relationships for the data shown in A. The rise in $[Cl]_i$ led to some positive shift of the curve on the voltage axis. Curves in A and B are Boltzmann-fits. For further analysis, cf. Table 2. Error bars indicate s.e.m.

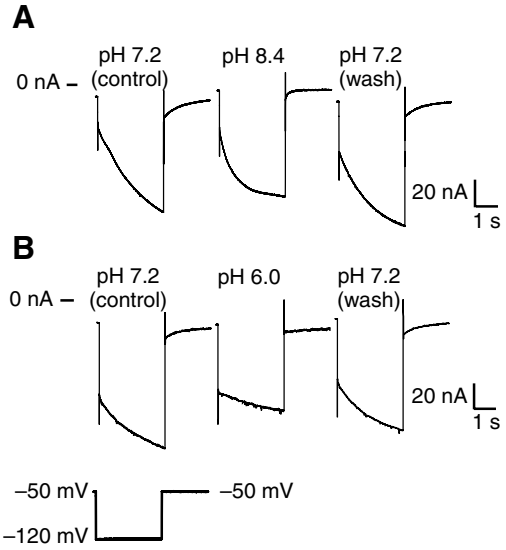

Fig. 6. Effects of pH changes on time course and amplitude of $I_{Cl,H}$. (A) A change from pH 7.2 to 8.4 leads to a faster time course of the hyperpolarisation-induced Cl^- current. The amplitude, obtained by extrapolating the current until it reached steady state, was somewhat reduced. Voltage jump was as shown in B. (B) At pH 6.0 the amplitude became greatly reduced. The time course of the current appears to be slowed, yet in fact it remained unaffected, as found on fitting double exponentials to the current traces. Both pH effects were rapid; they were recorded ≈1 min after changing the bath solution. The recordings labelled 'wash' were made 3 to 5 min after changing back to pH 7.2. For a more detailed analysis of these effects see Table 1.

[Fig. 10C; determined by differential interference contrast (DIC) and fluorescence microscopy]. The same experiments with antibodies pre-absorbed with the ClC-2 protein yielded no positive staining (Fig. 10C).

Discussion

Studies of ClC channels in invertebrates have started only recently and are presently restricted to the nematode *C. elegans* (Schriever et al., 1999; Nehrke et al., 2000; Rutledge et al., 2001) and the fruitfly *Drosophila melanogaster* (Ugarte et al., 2005; Flores et al., 2006). According to a phylogenetic similarity tree, of the six ClC genes in the nematode *C. elegans*, four are believed to code for plasma membrane channels (CeCLC-1 to -4) (Schriever et al., 1999) in contrast to only one of three in *Drosophila* (Dow and Davies, 2003). We have demonstrated the expression of this gene, DmClC-2, in larval muscles (Fig. 10). The plasma membrane ClC channels of either species are most closely related to the ClC-2 variant of mammalian ClCs, which activates on hyperpolarisation. Particular residues in the cytoplasmic linker between helix J and helix K (former nomenclature D7-D8) and in the N-terminal region that are highly relevant to this type of gating and its dependence on cell swelling or low extracellular pH (Jordt and Jentsch, 1997; Varela et al., 2002; Gründer et al., 1992) are partially conserved in DmClC-2 (see Figs S1, S2 in supplementary material), but not in CeCLC-1 to -4 (Schriever et al., 1999).

Basic characteristics of DmClC-2 currents in Drosophila muscle

The steady-state activation of the muscular currents (Table 2; with $[Cl^-]_i$=38 mmol l^{-1}) and of the DmClC-2 currents expressed in HEK-293 cells ($[Cl^-]_i$=35 mmol l^{-1}) (Flores et al., 2006) had similar voltages of half-maximal activation, i.e. $V_{0.5}$≈–120 mV in the former and –110 to –120 mV in the two splice variants of the latter. The slope factors determined for the muscular currents were around 10 mV, which is similar to the value determined in locust muscle (Walther and Zittlau, 1998). By contrast, the slope factor of ClC currents measured in *Drosophila* photoreceptors was around 5 mV [recalculated from Ugarte et al. (Ugarte et al., 2005)]. These figures are considerably smaller than that observed on heterologous expression of DmClC-2, namely ≈20 mV (Flores et al., 2006).

The voltage-dependence of activation of ClC-2 currents depends strongly on the internal Cl^- concentration (Staley, 1994; Pusch et al., 1999). In mammalian cells (Haug et al., 2003; Catalan et al., 2004) $V_{0.5}$ is shifted by about the same amount as E_{Cl} when $[Cl^-]_i$ is changed. As shown in the present work, *Drosophila* DmClC-2 channels show a similar dependence (Fig. 5B). This behaviour is considered a hallmark of ClC-2 currents (Pusch et al., 1999), and because it was also

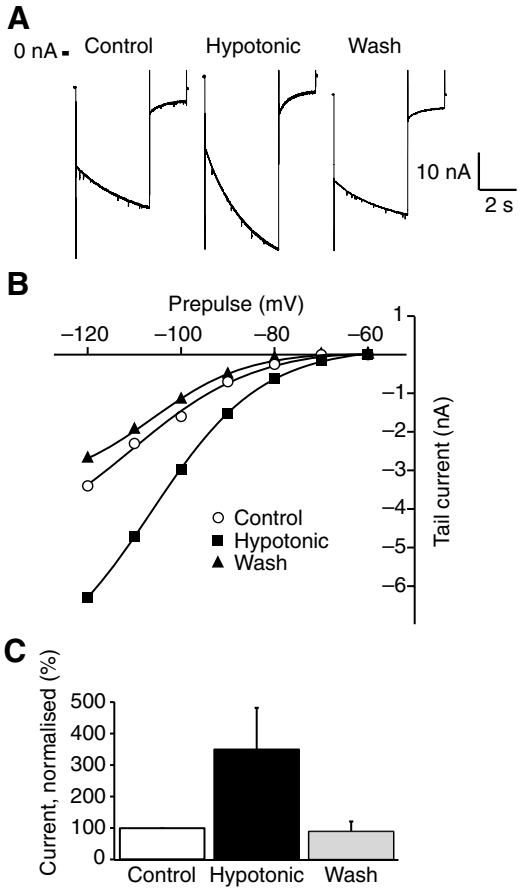

Fig. 7. Potentiation of $I_{Cl,H}$ in hypotonic saline. (A) Currents recorded from one fibre on jumping the voltage from –50 to –120 mV. The intervals between the different recording conditions lasted 8–10 min. (B) Amplitudes of tail currents following hyperpolarising prepulses as in A. Data from the same fibre as in A. The lines connecting the data points represent Boltzmann-fits with the following parameters, presented in the sequence control-hypotonic wash: I_{max}: 5.2, 8.5, 3.4 (nA); $V_{0.5}$: –110, –106, –106 (mV); k (slope factor): 13.1, 11.8, 10.0 (mV). (C) Mean osmotically induced increase in tail currents recorded after –120 mV prepulses as shown in A (f=4, l=2, N=4).

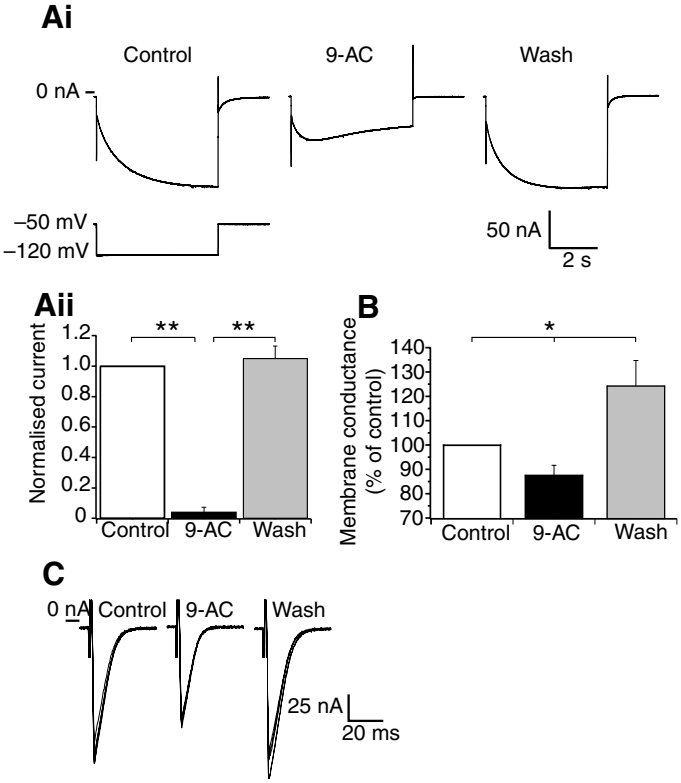

Fig. 8. Effect of 9-AC. (Ai) Representative recordings from one fibre performed 3 min (control), 8 min (9-AC) and 17 min after impaling the muscle fibre. 9-AC, at –120 mV, blocks $I_{Cl,H}$ in a time-dependent manner and reduces the tail current on jumping back to –50 mV. Prolonged washing led to almost full recovery of $I_{Cl,H}$. (Aii) Means and their standard errors of normalized $I_{Cl,H}$ from four experiments. (B) The effect of 1 mmol l^{-1} 9-AC on the resting membrane conductance measured by voltage ramps. 9-AC significantly lowered the membrane conductance of muscle fibres by approximately 20%. (C) Synaptic currents were consistently decreased by 1 mmol l^{-1} 9-AC to approximately 70% of the control value (N=4). This effect was reversed by washing with saline.

observed for the hyperpolarisation-dependent Cl^- current in snail neuron (Chesnoy-Marchais, 1983) and locust muscle (Walther and Zittlau, 1998) both currents are probably carried by ClC-2 channels, too.

There was, however, also a pronounced increase in maximal steady-state conductance when $[Cl^-]_i$ was raised (Fig. 5A), although we have to keep in mind that this observation rests on extrapolations of data. This chloride dependency seems to be not uncommon in plasma membrane ClC channels (e.g. Pusch et al., 1999), but it has not been demonstrated frequently and does, for example, not occur in the hippocampal ClC-2 currents studied by Staley et al. (Staley et al., 1996). A change in steady-state G_{max} with $[Cl^-]_i$ (larger than predicted from the constant field equation) was, however, found in *Aplysia* neurons and in locust skeletal muscle (Walther and Zittlau, 1998). Presently, we are not aware of a channel model that explicitly predicts this behaviour.

The time course of $I_{Cl,H}$ was rather variable but clearly slower than that of the DmClC-2 currents on heterologous expression: at –120 mV the two time constants describing the time course of activation were $\tau_1 \approx 1.8$ s and $\tau_2 \approx 3.5$ s in muscle, compared with approximately 0.1 s and 0.7 s, respectively, observed for DmClC-2 in HEK-293 cells [estimated from fig. 4 of Flores et al. (Flores et al., 2006)]. The time course of DmClC-2 currents in *Drosophila* photoreceptors measured from whole-cell recordings was even faster (Ugarte et al., 2005). It should be pointed out that in those investigations a fourfold higher internal Cl^- concentration was used. Discrepancies may also be expected if splice variant(s) of DmClC-2 are expressed in muscle, which could differ from those investigated in HEK cells (DmClC-2L and DmClC-2S) (Flores et al., 2006).

Like other ClC-2 currents (e.g. Jentsch et al., 2002; Clark et al., 1998; Duan et al., 2000), both the muscular and the photoreceptor Cl^- currents (Ugarte et al., 2005) were blocked by 9-AC with moderate efficiency. Block by extracellularly applied Zn^{2+} or Cd^{2+} was not observed in the current study. This may seem surprising because mammalian ClC-2 currents generally appear to be rather sensitive to both ions (e.g. Clark

et al., 1998; Kajita et al., 2000). In *Drosophila* photoreceptors Zn^{2+} blocked the Cl^- current, yet application was from the intracellular side (Ugarte et al., 2005). It remains to be seen whether the muscular current is sensitive to intracellularly applied Zn^{2+}, or whether a more alkaline pH may be required for the current to become susceptive (Arreola et al., 2002).

Modification of muscular DmClC-2 current by pH and osmolality

ClC-2 currents of mammals and *C. elegans* rise on acidification and decrease on alkalinisation of the extracellular pH (e.g. Jentsch et al., 2002; Rutledge et al., 2001). Arreola et al. showed a bimodal dependence of ClC-2 current on the extracellular proton concentration (Arreola et al., 2002), giving a bell-shaped characteristic with a maximum pH of around 6.5. The situation may be similar in *Drosophila* muscle because the magnitude of $I_{Cl,H}$ was reduced both at pH 6.0 and pH 8.4. Arreola et al. observed no effect on the time course of activation with pH changes between 8.0 and 6.5 but found a pronounced slowing at pH 6.0 (Arreola et al., 2002). In *Drosophila* muscle, an analogous pH dependence was observed (Table 1), although the situation deserves further clarification.

Potentiation of ClC-2 current by hypotonicity-induced cell swelling has been commonly observed (e.g. Clark et al., 1998; Gründer et al., 1992; Duan et al., 2000; Rutledge et al., 2001) and represents one of the characteristics of ClC-2 currents. The present work showed a considerable augmentation of $I_{Cl,H}$ that might be relevant for regulatory volume decrease as supported by experiments on insect cells (Xiong et al., 1999) and *Xenopus* oocytes (Furukawa et al., 1998). The potentiation was rather variable, which may be because of variations of $I_{Cl,H}$ control current. The effects in muscle fibres exhibiting a rather large control $I_{Cl,H}$ are presumably smaller compared with those with a small control $I_{Cl,H}$. This notion is supported by the findings of Clark et al. in rat superior cervical ganglion neurons (Clark et al., 1998) and Hall et al. in chick heart cells (Hall et al., 1995).

Possible function(s) of muscular DmClC-2 current

DmClC-2 also occurs in neuronal tissue (Fig. 9A) (Ugarte et al., 2005), is enriched in Malpighian tubules (Dow and Davies, 2003; Wang et al., 2004) and might be ubiquitously expressed like ClC-2 in mammals (e.g. Jentsch et al., 2002). A specific role, however, of a ClC-2 channel in insect muscle is not immediately clear. Because muscular tissue represents one of the largest compartments of the body, it may contribute significantly to homeostatic regulation of pH and osmolality. The dependence of muscular DmClC-2 currents on pH and their increase under hypotonic conditions would be important prerequisites for such a role. In general, the finding that ClC-2 channels open mainly at voltages more negative than E_{Cl} is believed to indicate that these channels serve the efflux of Cl^- ions. In *Drosophila* muscle, $I_{Cl,H}$ channels begin to open mainly at voltages approximately 30 mV more negative than E_{Cl} compared with figures of 10 to 15 mV in locust muscle (Walther and Zittlau, 1998) and *Aplysia* neuron (Chesnoy-Marchais, 1983) and around 0 mV in hippocampal neurons (Haug et al., 2003; Staley, 1994).

How large is the Cl^- conductance at the physiological resting potential of around –50 mV (Ball et al., 2003) in *Drosophila* muscle? Activation measurements of DmClC-2 currents in the expression system indicated that a fraction of the order of 10% of the channels does not deactivate even at voltages positive from E_{Cl} (Flores et al., 2006). From applications of the blocker 9-AC it can be deduced that in larval muscle there is a Cl^- conductance at the resting potential of the order of 0.05 μS, which represents some 20% of the total resting conductance (Fig. 8B). A resting Cl^- conductance of similar magnitude was indicated by preliminary ion substitution experiments (N=3) in which $[Cl^-]_o$ was reduced to 10% of the control. Thus, ClC-2 may be mainly responsible for the resting Cl^- conductance, although other types of Cl^- channels, of course, might also exist in muscle. The effective potentiation of neurally evoked contractions in *Drosophila* muscle by 9-AC (Fig. 9) has certainly to be attributed to the reduction of membrane resting conductance. This effect of 9-AC thus more than compensates its depressing action on synaptic currents (Fig. 8C), whereas the threshold for contraction (approximately –25 mV) seems not to be affected by 9-AC (authors' unpublished data).

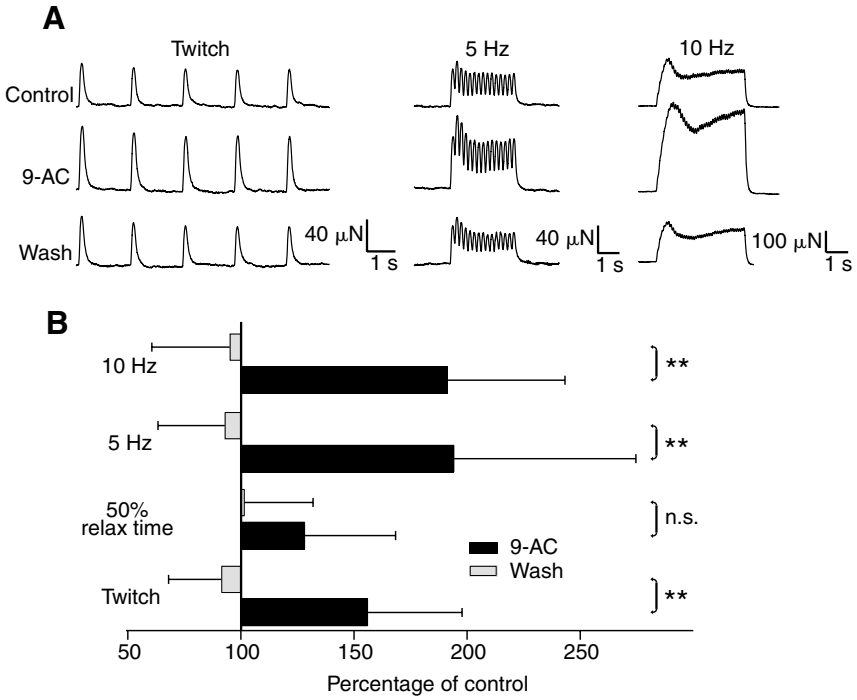

Fig. 9. Effect of 9-AC on stimulus evoked muscular contraction. (A,B) Muscular contractions were consistently augmented when 1 mmol l^{-1} 9-AC was applied to the bath. Washing with saline almost reversed this effect. The 9-AC effect was basically similar for single contractions (twitch) or tetanus (5 Hz, 10 Hz) contractions, although it seemed to be less pronounced for twitch contractions. However, no significant difference was detected between twitch and tetanus. 9-AC did not change the time course (50% relaxation time) of twitch contractions.

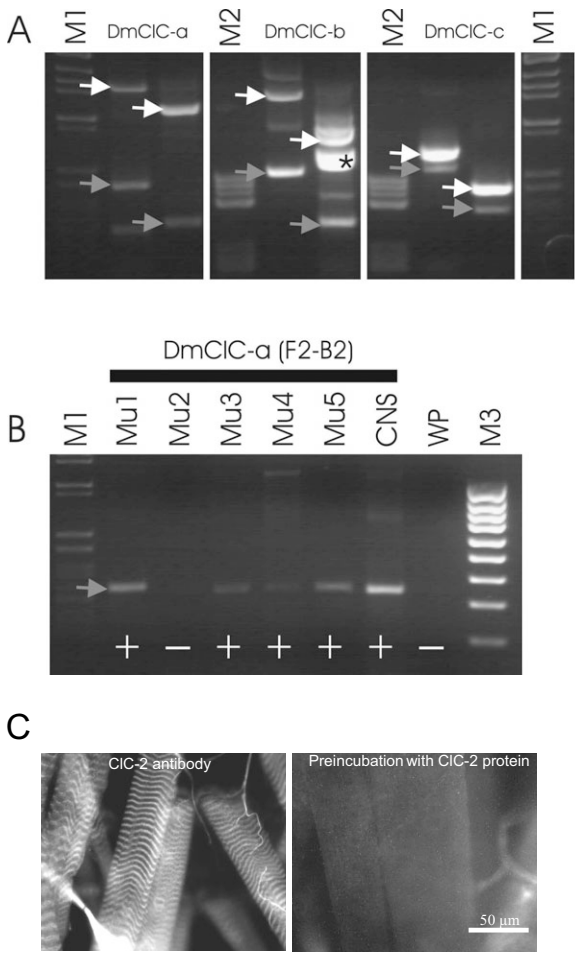

Fig. 10. RT-PCR analysis of the expression of ClC channels in *Drosophila melanogaster* muscle preparations. (A) RT-PCR analysis of body wall RNA preparations. Two independent PCR reactions were performed for each *Drosophila* ClC channel (primers F1-B1 in left lane and F2-B2 in right lane). (B) DmClC-a RT-PCR analysis (primers F2-B2) of five different pure muscle RNA preparations, Mu1-5 and CNS. Grey arrows indicate RT-PCR products; white arrows indicate PCR products amplified from genomic DNA; *, an unspecific amplification (as verified by DNA sequencing). DNA marker: M1, λDNA/*Eco*47I; M2, pBR322 DNA/*Bsu*RI; M3, 100 bp ladder; WP, water control. 'DmClC-a' corresponds to 'DmClC-2', which is chiefly used in the text and which has been introduced by Flores et al. (Flores et al., 2006). (C) Localisation of the ClC-2 channel in larval longitudinal muscles by immunohistochemistry showed distinct bands of antibody staining. ClC-2-positive staining corresponds to the Z-line of the sarcomere.

DmClC-2 may become functionally more relevant upon a physiologically induced rise of $[Cl^-]_i$. As shown above, even a small change should have major consequences because of the triple effect, namely a slight increase in driving force, a large increase in maximal conductance and a positive shift of the activation curve on the voltage axis. An increase in $[Cl^-]_i$ might occur secondary to high electrical activity and/or *via* ligand-mediated influx of Cl^- as previously discussed in detail for locust muscle (Walther and Zittlau, 1998). There are no GABA-receptors in *Drosophila* muscle (U.R., unpublished data), yet glutamate-dependent Cl^- currents have been demonstrated (Delgado et al., 1989).

Finally, there might be one or more modulators of $I_{Cl,H}$ as, for example, has been observed for the putative ClC-2 current in locust muscle. This current is enhanced by the biogenic amine octopamine (Walther and Zittlau, 1998), which acts *via* a rise of cAMP (cf. Evans, 1984). Also, for the putative ClC-2 current in *Aplysia* neurons (Chesnoy-Marchais, 1983) modulation by a biogenic amine and two neuropeptides have been described (Buttner and Siegelbaum, 2003; Lotshaw and Levitan, 1987). In *Drosophila* muscle, cAMP did not alter the Cl^- currents (U.R., unpublished data; *N*=5). However, a polyunsaturated fatty acid increased DmClC-2 currents in photoreceptors (Ugarte et al., 2005). There is a large number of neuropeptides and other potential modulators in *Drosophila* (Nässel, 2002; Hauser et al., 2006; Nässel and Homberg, 2006). Thus, future studies will have to show whether one or more of them modulates the muscular DmClC-2 current.

This work was supported by a grant of the Rudolf und Clothilde Eberhardt Stiftung to U.R. We thank Drs A. Meghigian and Th. Roeder for some helpful technical suggestions and Dr D. Wicher for his comments on the manuscript.

References

Arreola, J., Begenisich, T. and Melvin, J. E. (2002). Conformation-dependent regulation of inward rectifier chloride channel gating by extracellular protons. *J. Physiol.* **541**, 103-112.

Atwood, H. L., Govind, C. K. and Wu, C. F. (1993). Differential ultrastructure of synaptic terminals on ventral longitudinal abdominal muscles in *Drosophila* larvae. *J. Neurobiol.* **24**, 1008-1024.

Ball, R., Xing, B., Bonner, P., Shearer, J. and Cooper, R. L. (2003). Long-term in vitro maintenance of neuromuscular junction activity of *Drosophila* larvae. *Comp. Biochem. Physiol.* **134A**, 247-255.

Bretag, A. H. (1987). Muscle chloride channels. *Physiol. Rev.* **67**, 618-724.

Buttner, N. and Siegelbaum, S. A. (2003). Antagonistic modulation of a hyperpolarisation-activated Cl(–) current in *Aplysia* sensory neurons by SCP(B) and FMRFamide. *J. Neurophysiol.* **90**, 586-598.

Catalan, M., Niemeyer, M. I., Cid, L. P. and Sepulveda, F. V. (2004). Basolateral ClC-2 chloride channels in surface colon epithelium: regulation by a direct effect of intracellular chloride. *Gastroenterology* **126**, 1104-1114.

Chesnoy-Marchais, D. (1983). Characterization of a chloride conductance activated by hyperpolarisation in *Aplysia* neurons. *J. Physiol.* **342**, 277-308.

Clark, S., Jordt, S. E., Jentsch, T. J. and Mathie, A. (1998). Characterization of the hyperpolarisation-activated chloride current in dissociated rat sympathetic neurons. *J. Physiol.* **506**, 665-678.

Delgado, R., Barla, R., Latorre, R. and Labarca, P. (1989). L-glutamate activates excitatory and inhibitory channels in *Drosophila* larval muscle. *FEBS Lett.* **243**, 337-342.

Derst, C., Walther, C., Veh, R. W., Wicher, D. and Heinemann, S. H. (2006). Four novel sequences in *Drosophila* melanogaster homologous to the auxiliary Para sodium channel subunit TipE. *Biochem. Biophys. Res. Commun.* **339**, 939-948.

Dow, J. T. and Davies, S. A. (2003). Integrative physiology and functional genomics of epithelial function in a genetic model organism. *Physiol. Rev.* **83**, 687-729.

Duan, D., Ye, L., Britton, F., Horowitz, B. and Hume, J. R. (2000). A novel anionic inward rectifier in native cardiac myocytes. *Circ. Res.* **86**, E63-E71.

Elkins, T. and Ganetzky, B. (1988). The roles of potassium currents in *Drosophila* flight muscles. *J. Neurosci.* **8**, 428-434.

Erxleben, C. and Rathmayer, W. (1997). A dihydropyridine-sensitive voltage-dependent calcium channel in the sarcolemmal membrane of crustacean muscle. *J. Gen. Physiol.* **109**, 313-326.

Evans, P. D. (1984). The role of cyclic nucleotides and calcium in the mediation of the modulatory effects of octopamine on locust skeletal muscle. *J. Physiol.* **348**, 325-340.

Fahlke, C., Rudel, R., Mitrovic, N., Zhou, M. and George, A. L., Jr (1995). An aspartic acid residue important for voltage-dependent gating of human muscle chloride channels. *Neuron* **15**, 463-472.

Flores, C. A., Niemeyer, M. I., Sepulveda, F. V. and Cid, L. P. (2006). Two splice variants derived from a *Drosophila melanogaster* candidate ClC gene generate ClC-2-type Cl- channels. *Mol. Membr. Biol.* **23**, 149-156.

Fujita, S. C., Inoue, H., Yoshioka, T. and Hotta, J. (1987). Quantitative tissue isolation from *Drosophila* freeze-dried in acetone. *Biochem. J.* **243**, 97-104.
Furukawa, T., Ogura, T., Katayama, Y. and Hiraoka, M. (1998). Characteristics of rabbit ClC-2 current expressed in *Xenopus* oocytes and its contribution to volume regulation. *Am. J. Physiol*. **274**, C500-C512.
George, A. L., Jr, Bianchi, L., Link, E. M. and Vanoye, C. G. (2001). From stones to bones: the biology of ClC chloride channels. *Curr. Biol*. **11**, R620-R628.
Gho, M. and Mallart, A. (1986). Two distinct calcium-activated potassium currents in larval muscle fibres of *Drosophila melanogaster*. *Pflugers Arch*. **407**, 526-533.
Gielow, M. L., Gu, G. G. and Singh, S. (1995). Resolution and pharmacological analysis of the voltage-dependent calcium channels of *Drosophila* larval muscles. *J. Neurosci.* **15**, 6085-6093.
Gründer, S., Thiemann, A., Pusch, M. and Jentsch, T. J. (1992). Regions involved in the opening of CIC-2 chloride channel by voltage and cell volume. *Nature* **360**, 759-762.
Hall, S. K., Zhang, J. and Lieberman, M. (1995). Cyclic AMP prevents activation of a swelling-induced chloride-sensitive conductance in chick heart cells. *J. Physiol*. **488**, 359-369.
Haug, K., Warnstedt, M., Alekov, A. K., Sander, T., Ramirez, A., Poser, B., Maljevic, S., Hebeisen, S., Kubisch, C., Rebstock, J. et al. (2003). Mutations in CLCN2 encoding a voltage-gated chloride channel are associated with idiopathic generalized epilepsies. *Nat. Genet*. **33**, 527-532.
Hauser, F., Cazzamali, G., Williamson, M., Blenau, W. and Grimmelikhuijzen, C. J. (2006). A review of neurohormone GPCRs present in the fruitfly *Drosophila melanogaster* and the honey bee *Apis mellifera*. *Prog. Neurobiol*. **80**, 1-19.
Heidel, E. and Pflüger, H. J. (2006). Ion currents and spiking properties of identified subtypes of locust octopaminergic dorsal unpaired median neurons. *Eur. J. Neurosci.* **23**, 1189-1206.
Jan, L. Y. and Jan, Y. N. (1976). Properties of the larval neuromuscular junction in *Drosophila melanogaster*. *J. Physiol.* **262**, 189-214.
Jentsch, T. J., Pusch, M., Rehfeldt, A. and Steinmeyer, K. (1993). The ClC family of voltage-gated chloride channels, structure and function. *Ann. N. Y. Acad. Sci*. **707**, 285-293.
Jentsch, T. J., Lorenz, C., Pusch, M. and Steinmeyer, K. (1995). Myotonias due to CLC-1 chloride channel mutations. *Soc. Gen. Physiol. Ser.* **50**, 149-159.
Jentsch, T. J., Stein, V., Weinreich, F. and Zdebik, A. A. (2002). Molecular structure and physiological function of chloride channels. *Physiol. Rev*. **82**, 503-568.
Jordt, S. E. and Jentsch, T. J. (1997). Molecular dissection of gating in the ClC-2 chloride channel. *EMBO J.* **16**, 1582-1592.
Jurkat-Rott, K. and Lehmann-Horn, F. (2004). Ion channels and electrical properties of skeletal muscle. In *Myology* (ed. A. G. Engel and C. Franzini-Armstrong), pp. 203-223. New York: McGraw-Hill.
Kajita, H., Whitwell, C. and Brown, P. D. (2000). Properties of the inward-rectifying Cl- channel in rat choroid plexus: regulation by intracellular messengers and inhibition by divalent cations. *Pflugers Arch*. **440**, 933-940.
Kidokoro, Y. and Nishikawa, K. (1994). Miniature endplate currents at the newly formed neuromuscular junction in *Drosophila* embryos and larvae. *Neurosci. Res.* **19**, 143-154.
Koch, M. C., Steinmeyer, K., Lorenz, C., Ricker, K., Wolf, F., Otto, M., Zoll, B., Lehmann-Horn, F., Grzeschik, K. H. and Jentsch, T. J. (1992). The skeletal muscle chloride channel in dominant and recessive human myotonia. *Science* **257**, 797-800.
Littleton, J. T. and Ganetzky, B. (2000). Ion channels and synaptic organization: analysis of the *Drosophila* genome. *Neuron* **26**, 335-343.
Lotshaw, D. P. and Levitan, I. B. (1987). Serotonin and forskolin modulation of a chloride conductance in cultured identified *Aplysia* neurons. *J. Neurophysiol*. **58**, 922-939.
Nässel, D. R. (2002). Neuropeptides in the nervous system of *Drosophila* and other insects: multiple roles as neuromodulators and neurohormones. *Prog. Neurobiol.* **68**, 1-84.
Nässel, D. R. and Homberg, U. (2006). Neuropeptides in interneurons of the insect brain. *Cell Tissue Res.* **326**, 1-24.
Nehrke, K., Begenisich, T., Pilato, J. and Melvin, J. E. (2000). Into ion channel and transporter function. *Caenorhabditis elegans* ClC-type chloride channels: novel variants and functional expression. *Am. J. Physiol.* **279**, C2052-C2066.
Niemeyer, M. I., Cid, L. P., Zuniga, L., Catalan, M. and Sepulveda, F. V. (2003). A conserved pore-lining glutamate as a voltage- and chloride-dependent gate in the ClC-2 chloride channel. *J. Physiol.* **553**, 873-879.
Pape, H. C. (1996). Queer current and pacemaker: the hyperpolarisation-activated cation current in neurons. *Annu. Rev. Physiol*. **58**, 299-327.
Pedersen, T. H., de Paoli, F. and Nielsen, O. B. (2005). Increased excitability of acidified skeletal muscle: role of chloride conductance. *J. Gen. Physiol.* **125**, 237-246.
Petalcorin, M. I., Oka, T., Koga, M., Ogura, K., Wada, Y., Ohshima, Y. and Futai, M. (1999). Disruption of clh-1, a chloride channel gene, results in a wider body of *Caenorhabditis elegans*. *J. Mol. Biol.* **294**, 347-355.
Pusch, M. (2002). Myotonia caused by mutations in the muscle chloride channel gene CLCN1. *Hum. Mutat.* **19**, 423-434.
Pusch, M., Jordt, S. E., Stein, V. and Jentsch, T. J. (1999). Chloride dependence of hyperpolarisation-activated chloride channel gates. *J. Physiol*. **515**, 341-353.
Reuben, J. P., Girardier, L. and Grundfest, H. (1962). The chloride permeability of crayfish muscle fibres. *Biol. Bull. Mar. Biol. Lab.* **123**, 509-510.
Rutledge, E., Bianchi, L., Christensen, M., Boehmer, C., Morrison, R., Broslat, A., Beld, A. M., George, A. L., Greenstein, D. and Strange, K. (2001). CLH-3, a ClC-2 anion channel ortholog activated during meiotic maturation in C. elegans oocytes. *Curr. Biol.* **11**, 161-170.
Schriever, A. M., Friedrich, T., Pusch, M. and Jentsch, T. J. (1999). CLC chloride channels in *Caenorhabditis elegans*. *J. Biol. Chem.* **274**, 34238-34244.
Singh, S. and Wu, C. F. (1999). Ionic currents in larval muscles of *Drosophila*. *Int. Rev. Neurobiol.* **43**, 191-220.
Staley, K. (1994). The role of an inwardly rectifying chloride conductance in postsynaptic inhibition. *J. Neurophysiol.* **72**, 273-284.
Staley, K., Smith, R., Schaack, J., Wilcox, C. and Jentsch, T. J. (1996). Alteration of $GABA_A$ receptor function following gene transfer of the CLC-2 chloride channel. *Neuron* **17**, 543-551.
Steinmeyer, K., Ortland, C. and Jentsch, T. J. (1991a). Primary structure and functional expression of a developmentally regulated skeletal muscle chloride channel. *Nature* **354**, 301-304.
Steinmeyer, K., Klocke, R., Ortland, C., Gronemeier, M., Jockusch, H., Grunder, S. and Jentsch, T. J. (1991b). Inactivation of muscle chloride channel by transposon insertion in myotonic mice. *Nature* **354**, 304-308.
Strange, K. (2002). Of mice and worms: novel insights into ClC-2 anion channel physiology. *News Physiol. Sci.* **17**, 11-16.
Suzuki, M., Morita, T. and Iwamoto, T. (2006). Diversity of Cl^- channels. *Cell. Mol. Life Sci.* **63**, 12-24.
Thiemann, A., Grunder, S., Pusch, M. and Jentsch, T. J. (1992). A chloride channel widely expressed in epithelial and non-epithelial cells. *Nature* **356**, 57-60.
Tsunoda, S. and Salkoff, L. (1995). Genetic analysis of *Drosophila* neurons: Shal, Shaw, and Shab encode most embryonic potassium currents. *J. Neurosci.* **15**, 1741-1754.
Ueda, A. and Kidokoro, Y. (1996). Longitudinal body wall muscles are electrically coupled across the segmental boundary in the third instar larva of *Drosophila melanogaster*. *Invert. Neurosci.* **1**, 315-322.
Ugarte, G., Delgado, R., O'Day, P. M., Farjah, F., Cid, L. P., Vergara, C. and Bacigalupo, J. (2005). Putative ClC-2 chloride channel mediates inward rectification in *Drosophila* retinal photoreceptors. *J. Membr. Biol*. **207**, 151-160.
Varela, D., Niemeyer, M. I., Cid, L. P. and Sepulveda, F. V. (2002). Effect of an N-terminus deletion on voltage-dependent gating of the ClC-2 chloride channel. *J. Physiol.* **544**, 363-372.
Walther, C. and Zittlau, K. E. (1998). Resting membrane properties of locust muscle and their modulation II. Actions of the biogenic amine octopamine. *J. Neurophysiol*. **80**, 785-797.
Walther, C., Zittlau, K. E., Murck, H. and Voigt, K. (1998). Resting membrane properties of locust muscle and their modulation I. Actions of the neuropeptides YGGFMRFamide and proctolin. *J. Neurophysiol*. **80**, 771-784.
Wang, J., Kean, L., Yang, J., Allan, A. K., Davies, S. A., Herzyk, P. and Dow, J. A. (2004). Function-informed transcriptome analysis of *Drosophila* renal tubule. *Genome Biol*. **5**, R69.
Wicher, D., Walther, C. and Wicher, C. (2001). Non-synaptic ion channels in insects: basic properties of currents and their modulation in neurons and skeletal muscles. *Prog. Neurobiol*. **64**, 431-525.
Wu, C. F. and Haugland, F. N. (1985). Voltage clamp analysis of membrane currents in larval muscle fibres of *Drosophila*: alteration of potassium currents in Shaker mutants. *J. Neurosci*. **5**, 2626-2640.
Xiong, H., Li, C., Garami, E., Wang, Y., Ramjeesingh, M., Galley, K. and Bear, C. E. (1999). ClC-2 activation modulates regulatory volume decrease. *J. Membr. Biol.* **167**, 215-221.
Zhang, Y., Oliva, R., Gisselmann, G., Hatt, H., Guckenheimer, J. and Harris-Warrick, R. M. (2003). Overexpression of a hyperpolarization-activated cation current (Ih) channelgene modifies the firing activity of identified motor neurons in a small neural network. *J. Neurosci.* **27**, 9059-9067.